DOI: 10.1002/ejic.200500753

Binuclear Mixed Valence Oxovanadium(IV/V) Complexes Containing a $[OV^{IV}(\mu\text{-}O_{oxo})(\mu\text{-}O_{phen})V^{V}O]^{2+}$ Core: Synthesis, EPR Spectra, Molecular and Electronic Structure

Amrita Mondal,[a] Sucharita Basak,[a] Sumana Sarkar,[a] Deepak Chopra,[b] Ranjan Das,[c] and Kajal Krishna Rajak*[a]

Keywords: Vanadium / Oxovanadium complexes / Mixed valence

Binuclear mixed valence oxovanadium(IV/V) complexes of general formula $[V_2O_3L]$ containing a $[OV^{IV}(\mu\text{-}O_{oxo})(\mu\text{-}O_{phen})V^{V}O]^{2+}$ core have been synthesised using conformationally labile N_4O_3-coordinating heptadentate ligands (H_3L). The X-ray structure of one complex has been examined. Solution EPR spectra revealed that the unpaired electron of the complexes is delocalised between the two vanadium centres. The simulated EPR spectrum of one complex confirms this experimental observation. DFT studies have been performed using crystallographic coordinates in order to obtain further insight into the electronic structure of this type of molecule.

Introduction

The chemistry of mixed valence vanadium complexes has been of considerable interest. The main interest arises from the complete or partial delocalisation of the single 3d electron of the vanadium(IV) over both vanadium centres or its complete localisation on one vanadium centre. A sizeable number of oxo-bridged binuclear mixed valence oxovanadium(IV/V) complexes have been cited in the literature[1–14] and depending on the geometry of $[V_2O_3]^{3+}$ core, the structurally characterised mixed valence binuclear complexes have been classified into several categories. For the $[V_2O_3]^{3+}$ core, containing a linear V–O–V bridge[1a,2,5,10,12,13] with the terminal oxo groups in mutual *trans* position, delocalisation is anticipated because of significant metal d_{xy} orbital overlap with the p_x orbital of the oxo bridge. Schulz et al.[7] reported that for the nearly *trans* V=O groups with a bent V–O–V moiety, the delocalisation of the odd electron between the two vanadium centres depends on the pi-donating ability of the equatorial ligands. Localised electronic structures have also been documented[6] for angular V–O–V moieties with *syn* or *twist* V=O groups, which probably occur due to insufficient overlap between the metal d_{xy} orbitals.

Recently we have found[15] complete delocalisation of the unpaired electron between the two vanadium atoms in a mixed bridged mixed valence species containing the $[OV^{IV}(\mu\text{-}O_x)(\mu\text{-}O_{phen})V^{V}O]^{2+}$ moiety, which has an angular V–O–V group and nearly *syn* V=O groups. However the reason for the delocalisation of the odd electron is not clear. Thus, further studies of this type of system are required to allow for a better understanding of the behaviour of the unpaired electron.

In connection with our previous work,[15] herein we describe the synthesis of a series of mixed bridged mixed valence binuclear oxovanadium(IV/V) complexes incorporating N_4O_3-coordinating heptadentate ligands. The crystal structure of one representative case is reported. A simulated EPR spectrum is found to be similar to the EPR spectra of the complexes observed in solution at room temperature. In addition, DFT calculations have enabled us to understand qualitatively the nature of the delocalisation of the unpaired electron.

Results and Discussion

In this paper four heptadentate ligands H_3L^7–H_3L^{10} (general abbreviation, H_3L) have been used (Scheme 1).

Treatment of a solution of $VO(acac)_2$ in acetone under air with the heptadentate ligands in a 2:1 ratio afforded green coloured complexes with the general formula $[V^{IV}V^{V}O_2L]$ in good yields. The oxygen in the air is believed to act as the oxidant in this synthesis. The data for the characterisation of these binuclear mixed valence species are listed in the experimental section. All the compounds display a strong V=O stretch near 950 cm^{-1}in their IR spectra, and the V–O–V vibration occurs near 752 cm^{-1}. The green solution of the complexes absorb at ca. 1030 and ca. 660 nm

[a] Inorganic Chemistry Section, Department of Chemistry, Jadavpur University,
Kolkata 700032, India
E-mail: kajalrajak@hotmail.com
[b] Solid State and Structural Chemistry Unit, Indian Institute of Science,
Bangalore 560012, India
[c] Department of Chemical Sciences, Tata Institute of Fundamental Research,
Mumbai, India

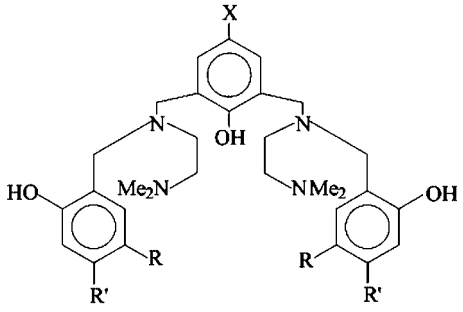

X = CH_3, R = H, R' = H:	H_3L^1	$[V_2O_3L^1]$
X = Cl, R = H, R' = H:	H_3L^7	$[V_2O_3L^7]$
X = Cl, R = Me, R' = H:	H_3L^8	$[V_2O_3L^8]$
X = Cl, R = Cl, R' = H:	H_3L^9	$[V_2O_3L^9]$
X = Cl, R = Cl, R' = Me:	H_3L^{10}	$[V_2O_3L^{10}]$

Scheme 1.

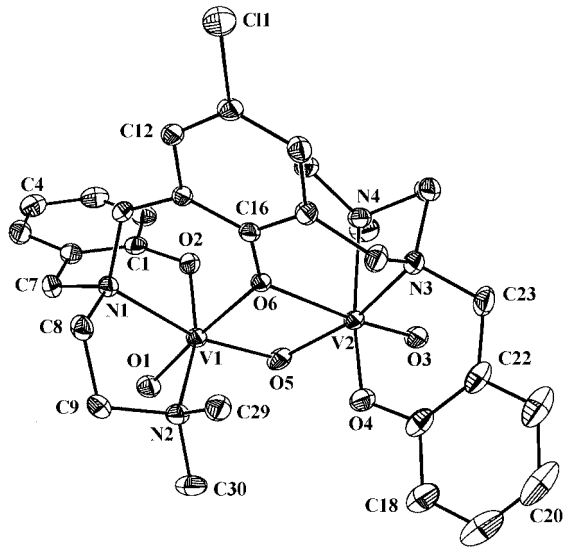

Figure 1. Perspective view and atom labeling scheme for $[V_2O_3L^7]$ CH_2Cl_2. The solvent molecule is excluded. All non-hydrogen atoms are represented by 30% thermal probability ellipsoids.

respectively. The band near 1030 nm in their UV/Vis spectra is assigned to the inter valence charge transfer transition,[15] and the absorption at 660 nm is due to ligand field excitation. The complexes exhibit an irreversible anodic response near 0.45 V vs. SCE. The stabilisation of the mixed valence oxovanadium(IV/V) binuclear species by the trianionic heptadentate ligand is reflected in the irreversible $[OV^V(\mu\text{-}O_{oxo})(\mu\text{-}O_{phen})V^VO]^{3+}$ – $[OV^{IV}(\mu\text{-}O_x)(\mu\text{-}O_{phen})\text{-}V^VO]^{2+}$ anodic response. All the compounds are paramagnetic, and the magnetic moment value is, $\mu \approx 1.75$ BM per molecule.

Crystal Structure

The X-ray structure of **1** has been determined, and the molecular structure is shown in Figure 1. Selected inter atomic distances and bond angles relevant to the coordination sphere are given in Table 1.

In **1** the vanadium centres are linked asymmetrically by a bridging oxygen atom, O5, and the central phenolato oxygen, O6. The V1–O5–V2 and V1–O6–V2 angles are 116.11(10)° and 91.79(7)° respectively. The geometry of each vanadium atom appears to be distorted octahedral. In the VO_4N_2 environment, the V=O, V–O and V–N bond lengths are as expected[15] and are in the ranges of 1.605–1.615 Å, 1.798–2.212 Å and 2.188–2.251 Å respectively. In the octahedral coordination environment, the tripodal nitrogen atom (N1 for V1 and N3 for V2) is *trans* to the O5 atom, while the terminal nitrogen atoms (N2 and N4) occupy positions *trans* to the terminal phenoxide groups (O2 and O4). The V2–O4 [1.871 (2) Å], V2–O5 [1.885 (2) Å] and V2–O6 [2.212 (2) Å] bond lengths are slightly longer than the respective V1–O2 [1.838 (2) Å], V1–O5 [1.798 (2) Å] and V1–O6 [2.140 (2) Å] bonds. The V1–N bond lengths are slightly longer than the V2–N distances, and this can be ascribed to the short V1–O2 and V1–O5 bonds.

Table 1. Selected bond lengths [Å] and angles (°) for $[V_2O_3L^7]$ CH_2Cl_2.

Distances			
V1–O1	1.605(2)	V2–O3	1.615(2)
V1–O2	1.838(2)	V2–O4	1.871(2)
V1–O5	1.798(2)	V2–O5	1.885(2)
V1–O6	2.140(2)	V2–O6	2.212(2)
V1–N1	2.238(2)	V2–N3	2.188(3)
V1–N2	2.251(3)	V2–N4	2.231(3)
V1···V2	3.125(5)		
Angles			
O1–V1–O2	98.53(10)	O3–V2–O4	97.08(11)
O1–V1–O5	104.65(10)	O3–V2–O5	104.54(11)
O1–V1–O6	169.44(10)	O3–V2–O6	171.63(10)
O1–V1–N1	94.36(10)	O3–V2–N3	98.39(11)
O1–V1–N2	85.41(10)	O3–V2–N4	85.16(10)
O2–V1–O5	95.12(10)	O4–V2–O5	89.69(10)
O2–V1–O6	91.42(8)	O4–V2–O6	91.22(9)
O2–V1–N1	82.85(9)	O4–V2–N3	86.46(10)
O2–V1–N2	159.60(9)	O4–V2–N4	165.27(11)
O5 –V1–O6	77.80(8)	O5–V2–O6	74.28(8)
O5–V1–N1	160.96(9)	O5–V2–N3	157.05(9)
O5–V1–N2	103.28(10)	O5–V2–N4	103.89(10)
O6–V1–N1	83.31(8)	O6–V2–N3	83.18(8)
O6–V1–N2	84.04(8)	O6–V2–N4	87.10(8)
N1–V1–N2	76.87(9)	N3–V2–N4	78.81(10)
V1–O5–V2	116.11(10)	V1–O6–V2	91.79(7)

EPR Spectra

EPR spectra of the complexes were recorded at 300 K and 77 K. Resonance parameters are shown in Table 2.

The complexes exhibit 15 nearly equally spaced lines, with isotropic structure, in dichloromethane solution (Figure 2, a). The 15 line spectrum arises from the hyperfine interaction of the unpaired electron with the two vanadium

Table 2. EPR spectral data.

Complex	Matrix	g_{iso}	$A_{iso}\times10^4$ [cm^{-1}]	$g_{\parallel}$	$g_{\perp}$	g_{av}[a]	$A_{\parallel}\times10^4$ [cm^{-1}]	$A_{\perp}\times10^4$ [cm^{-1}]	A_{av}[b]$\times10^4$ [cm^{-1}]
	CH_2Cl_2, 300 K	1.974	49.3						
$[V_2O_3L^7]$	CH_2Cl_2/toluene, 77 K								
	solid, 77 K	1.984		1.984	1.966	1.972	168.8	66.5	100.2
	CH_2Cl_2, 300 K								
$[V_2O_3L^8]$	CH_2Cl_2/toluene, 77 K	1.984	51						
	solid, 77 K			1.972	1.986	1.981	169.2	69.9	103
		1.989							
	CH_2Cl_2, 300 K								
$[V_2O_3L^9]$	CH_2Cl_2/toluene, 77 K	1.972	48.1						
	solid, 77 K			1.973	1.982	1.979	166.9	62.35	97.2
		1.986							
	CH_2Cl_2, 300 K								
$[V_2O_3L^{10}]$	CH_2Cl_2/toluene, 77 K	1.977	50.2						
	solid, 77 K			1.946	1.997	1.980	164	68.75	100.5
		1.985							

[a] $g_{av} = {}^1/_3[2\,g_{\perp} + g_{\parallel}]$. [b] $A_{av} = {}^1/_3[2A_{\perp} + A_{\parallel}]$.

nuclei (nuclear spin $I = 7/2$), which appear to be equivalent on the EPR timescale. The difference in the separation of the hyperfine lines at the lowest and highest fields is less than 2 gauss, suggesting that the second order shift[16] in the line position is small. We neglected this small shift, and determined the isotropic hyperfine coupling constant due to vanadium to be 49.3 ± 0.2 G. In the same way, neglecting the second order shift, the centre of the EPR spectrum was assumed to be the centre of the middle hyperfine line, and the g value for the complex was determined to be 1.9741 ± 0.0005. The isotropic coupling constant and the g value are typical for binuclear complexes,[15] and the value of the isotropic hyperfine coupling constant is about half of the value observed in oxovanadium(IV) complexes.[17] This indicates that in solution at 300 K, the single unpaired electron is shared by the two vanadium nuclei. The observed line width in not same for all the hyperfine lines. The dependence of the line width on the hyperfine lines of the EPR spectrum in solution has been modelled theoretically, using a model that incorporates incomplete motional narrowing, the anisotropic g-tensor, and hyperfine tensor interactions.[18,19] Using the Kivelson's model[18] the line width, ΔH, of a hyperfine line associated with the nuclear spin component M_I is given as equation (2) in ref.[20]

Where the parameters α, β, γ and δ are functions of the principal values of the g-tensor, hyperfine coupling tensor, and rotational correlation time. The line width expression given in [Equation (1)] has been highly successful in explaining the variation in the widths of the EPR lines in the spectrum of vanadyl acetylacetonate in toluene,[20] and has been used to obtain the anisotropic EPR parameters from solution spectra of copper complexes.[21,22] We have assumed that Equation 1 is approximately applicable to our binuclear complex, and have simulated the EPR spectrum based on this line width expression with $M_I = -7, -6, \ldots, +6, +7$, corresponding to the two equivalent vanadium nuclei. The simulated spectrum is shown in Figure 2 (b). Here we simply note that the simulated spectrum reproduces the

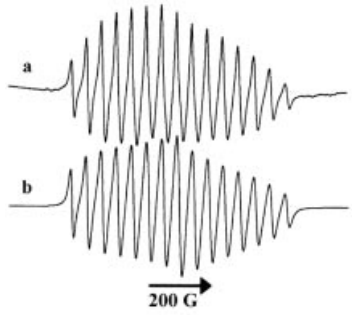

Figure 2. EPR spectra for $[V_2O_3L^7]$ (a) in DCM at 300 K. Instrument settings: microwave frequency, 9.45385 GHz; microwave power, 2.0 mW; modulation frequency, 100 kHz; modulation amplitude, ca. 1 G. (b) Simulated EPR spectrum using isotropic hyperfine coupling constant = 49.3 ± 0.2 G, and Kivelson's parameters α = 21.21 G, β = 0.2943 G, γ = –0.1538 and δ = 0.0007 G.

essential features of the experimental EPR spectrum of the binuclear complex at room temperature.

$$\Delta H = \alpha + \beta M_I + \gamma M_I^2 + \delta M_I^3 \quad (1)$$

The complexes display axial spectra at 77 K (Figure 3). The hyperfine structure can be attributed to the coupling of the unpaired electron to a single ^{51}V centre ($I = 7/2$), at least on the EPR timescale.[6,8]

In frozen solution (77 K) and fluid solution (300 K) the spectral parameters are related by the following equations:[23]

$g_{av} \approx g_{iso}$

$A_{av} \approx 2A_{iso}$

From the above relationships it may be deduced that the unpaired electron is equally delocalised between the two vanadium atoms, at least on the X-band EPR timescale, and the complexes behave as class III type[5,24,25] mixed valance species at room temperature.

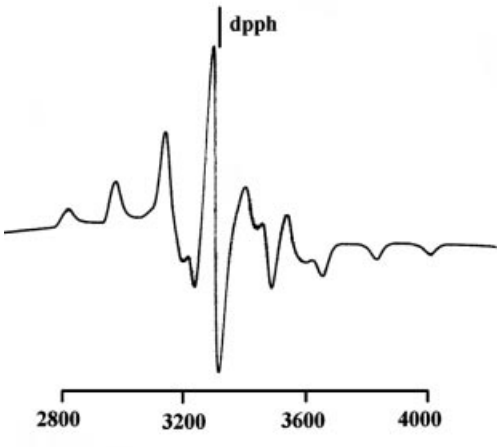

Figure 3. EPR spectra for $[V_2O_3L^7]$ in DCM/toluene at 77 K. Instrument settings: microwave frequency, 9.1 GHz; microwave power, 30 dB; modulation frequency, 100 kHz; modulation amplitude, 12.5 G; sweep centre, 3200 G.

DFT Study

DFT calculation have been performed on the full molecular structure using the crystallographic coordinates for $[V_2O_3L^7]$ and the previously reported $[V_2O_3L^1]$ complex[15] (ligand H_3L^1 is shown in Scheme 1) in order to get a better insight into the electronic structure of μ-oxo μ-phenoxo bridged binuclear oxovanadium(IV/V) complexes. The spin density, singly occupied molecular orbital (SOMO), and the lowest unoccupied molecular orbital (LUMO) plots for the complexes are shown in Figure 4, Figure 5 and Figure 6 respectively.

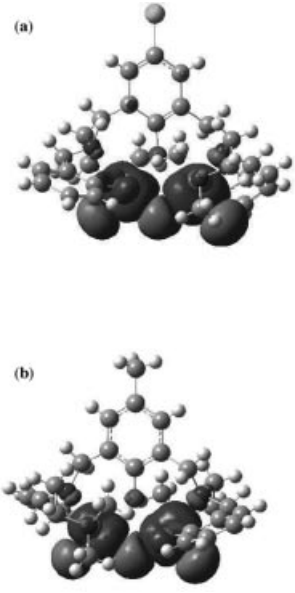

Figure 4. Spin density plots (a). $[V_2O_3L^7]$ (b). $[V_2O_3L^1]$.

The spin density population of the electron between the two vanadium atoms is 0.5700 and 0.4300 for $[V_2O_3L^7]$, and 0.5664 and 0.4336 for $[V_2O_3L^1]$. It is clear from the spin density plots (Figure 4) that the unpaired electron is delocalised between the two vanadium centres.

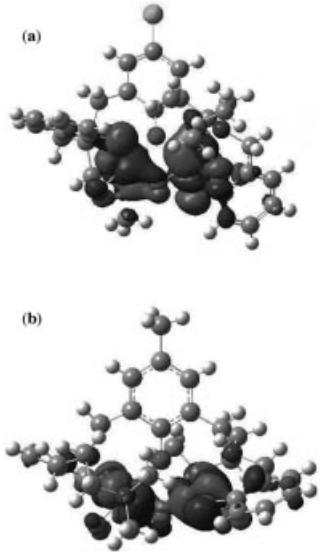

Figure 5. SOMO plots (a). $[V_2O_3L^7]$ (b). $[V_2O_3L^1]$.

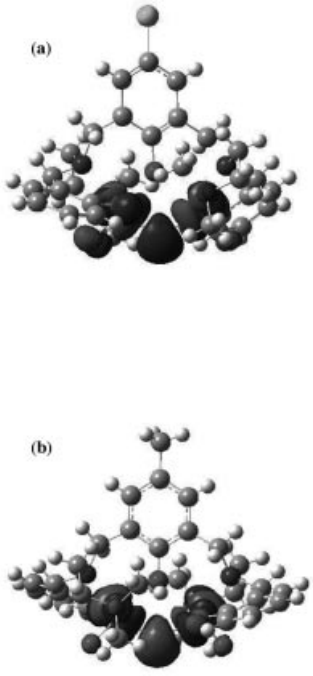

Figure 6. LUMO plots (a). $[V_2O_3L^7]$ (b). $[V_2O_3L^1]$.

It is interesting to note that the bridging oxo oxygen atom takes part in the construction of the SOMO, while the contribution of the bridging phenoxy oxygen to the SOMO is zero (Figure 5). The p_z orbital of the bridging oxo oxygen atom interacts with the d_{xz} orbital of the vanadium atoms asymmetrically in the $[V_2O_3L^7]$ complex, and symmetrically in the $[V_2O_3L^1]$ complex. These results are consistent with the $V–O_{oxo}–V$ bond lengths observed in these complexes. It is found from the LUMO plots that the bridging oxo oxygen (Figure 6) and the bridging phenoxy group do not in-

teract with the metal orbital. The above results suggest that the delocalisation of the electron between the two vanadium centres takes place via a d_{xz}–p_z–d_{xz} super exchange pathway in the ground state.

In summary, DFT studies reveal that in case of binuclear mixed valence oxovanadium(IV/V) complexes containing a $[OV^{IV}(\mu\text{-}O_{oxo})(\mu\text{-}O_{phen})V^{V}O]^{2+}$core with a bent V–O–V moiety, only the bridging oxo group is responsible for the unpaired electron delocalisation, and as such the delocalisation occurs via a d_{xz}–p_z–d_{xz} super exchange pathway.

Conclusion

Binuclear mixed valence oxovanadium(IV/V) complexes containing the $[OV^{IV}(\mu\text{-}O_{oxo})(\mu\text{-}O_{phen})V^{V}O]^{2+}$ moiety have been synthesised using N_4O_3-coordinating heptadentate ligands. In $[V_2O_3L^7]$, the V1–O5–V2 moiety is angular, and the V1–O5 and V2–O5 bond lengths are slight different [V1–O5 = 1.798(2) and V2–O5 = 1.885(2) Å]. Solution EPR spectra reveal that the unpaired electron is delocalised between the two vanadium atoms, which is attested by the simulated EPR spectrum. We have also found some important trends in the electronic structure, and hence in the behaviour of the unpaired electron, from the DFT studies. DFT calculations show that the bridging phenoxo group has no role to play in the electron delocalisation. Although the V–O–V group is angular, the delocalisation in such systems is anticipated to occur via an d_{xz}–p_z–d_{xz} exchange pathway involving the oxo oxygen atom.

Experimental Section

Materials: Bis(acetylacetonato)oxovanadium(IV)[26] and the ligands[27] were prepared as reported in the literature. All the starting chemicals were analytically pure and used without further purification, and the solvents were purified by standard procedures.[28]

Physical Measurements: UV/Vis spectra were recorded on a Perkin–Elmer LAMBDA 25 spectrophotometer, and IR spectra were measured with a Perkin–Elmer L-0100 spectrometer. Electrochemical measurements were performed (acetonitrile solution) on a CH 620A electrochemical analyzer using a platinum electrode. Tetraethylammonium perchlorate (TEAP)[29] was used as the supporting electrolyte, and the potentials are referenced to the standard calomel electrode (SCE) without junction correction. Magnetic susceptibilities were measured on a PAR-155 vibrating-sample magnetometer.

The room temperature solution EPR spectra were recorded for **1** in the following manner: the complex (ca. 10 mM in dichloromethane) was placed in a glass tube, and degassed by repeated freeze-pump-thaw cycles with a vacuum line working at a pressure of about 10^{-4} Torr., and then sealed off. This sealed sample was used for recording the CW-EPR spectrum at room temperature, using a home-built EPR spectrometer,[30] which was further modified.[31] Low microwave power (ca. 2 mW) and 100 kHz magnetic field modulation (ca. 1 gauss) were used to avoid distortion of the EPR lines. A proton NMR magnetometer was used to calibrate the scan range of the magnetic field. An Agilent frequency counter, model 53181A, equipped with a highly stable oven-controlled time base, was used to measure the microwave and NMR frequencies. For determining the g value of the complex, a very small amount of DPPH powder ($g = 2.0037 \pm 0.0002$)[32] was attached to the outside wall of the sealed sample, and the EPR spectrum of the complex with DPPH was recorded.

The room temperature solution EPR spectra of the other complexes, and the low temperature spectra for all the complexes, were recorded on a Varian E-109C X-band spectrometer. Elemental analyses (C, H, N) were performed on a Perkin–Elmer 2400 Series II elemental analyzer.

DFT Calculation: DFT calculations were performed using the Gaussian-03 program.[33] The complexes were described in the unrestricted formalism using the B3LYP hybrid density function in combination with a standard 3-21 G basis set.

Crystallographic Studies: Single crystals of suitable quality for single-crystal X-ray diffraction studies were grown by the slow diffusion of hexane into a dichloromethane solution containing $[V_2O_3L^7]\,CH_2Cl_2$. The X-ray intensity data were measured at 293 K on a Bruker AXS SMART APEX CCD diffractometer (Mo-K_α, λ = 0.71073 Å). The detector was placed at a distance of 6.03 cm from the crystal. A total of 606 frames were collected over a scan width of 0.3° at different settings of φ. The data were reduced with SAINTPLUS[34] and an empirical absorption correction was applied using the SADABS package.[24] Vanadium atoms were located by Direct Methods, and the rest of the non-hydrogen atoms emerged from successive Fourier syntheses. SHELXL-97[35] was used for structure solution, and for full-matrix least-squares structure refinement on F^2. All non-hydrogen atoms were refined anisotropically. All the hydrogen atoms were included at calculated positions. The dichloromethane solvent molecule is disordered over two positions. The disorder was modelled using the PART instruction in SHELXTL, with an initial occupancy of 0.5, which after refinement gave a final value of 0.583(5). Molecular structure plots were drawn using ORTEP.[36] Relevant crystal data are given in Table 3.

Table 3. Crystal data and structure refinement parameters for $[V_2O_3L^7]\cdot CH_2Cl_2$.

$[V_2O_3L^7]\cdot CH_2Cl_2$	
Formula	$C_{31}H_{40}Cl_3N_4O_6V_2$
Formula weight	772.90
Crystal system	monoclinic
Space group	$P2_1/c$
a [Å]	16.181(3)
B [Å]	13.986(3)
c [Å]	15.024(3)
β [°]	97.16(3)
V [Å^3]	3373.6(12)
T [K]	293(2)
Z	4
$D_{calcd.}$ (mg·m^{-3})	1.522
μ [mm^{-1}]	0.841
R_1,[a] wR_2[b] [$I > 2\sigma(I)$]	0.0490, 0.1121
R_1,[a] wR_2[b] [all]	0.0616, 0.1196
R_{int}, R_{sigma}	2.65, 2.47
G.O.F on F^2	1.058

[a] $R_1 = \Sigma||F_o| - |F_c||/\Sigma|F_o|$. [b] $wR_2 = [\Sigma w(F_o^2 - F_c^2)^2/\Sigma w(F_o^2)^2]^{1/2}$.

CCDC-281762 contains the supplementary crystallographic data for this paper. These data can be obtained free of charge from The Cambridge Crystallographic Data Centre via www.ccdc.cam.ac.uk/data_request/cif.

Synthesis of Complexes: The complexes were prepared by the same general method. Details are given here for a representative case.

$[V_2O_3L^7]$: To a stirred solution of $[VO(acac)_2]$ (0.10 g, 0.37 mmol) in 20 mL acetone was added the H_3L^7 ligand (0.098 g, 0.19 mmol). The reaction mixture was then stirred for 2 h at ambient temperature in air, and a green precipitate separated from the solution. The solution was filtered, washed with acetone, and then dried in vacuo over fused calcium chloride. Yield: 0.116 g (90%). $C_{30}H_{38}ClN_4O_6V_2$ (687.5): calcd. C 52.36, H 5.53, N 8.15; found: C 52.61, H 5.70, N 8.31. UV/Vis (CH_2Cl_2): λ_{max} (ε) = 1031 nm (255 M^{-1} cm^{-1}); 640 (700). IR (KBr): ν(V=O) 950, ν(V–O–V) 752 cm^{-1}. E_{pa} ($[OV^V(\mu\text{-}O_{oxo})(\mu\text{-}O_{phen})V^VO]^{3+}/[OV^{IV}(\mu\text{-}O_x)(\mu\text{-}O_{phen})V^VO]^{2+}$): +0.56 V (irr). μ_{eff} = 1.76 BM.

$[V_2O_3L^8]$: Yield: 0.117 g (87%). $C_{32}H_{42}ClN_4O_6V_2$ (701.5): calcd. C 53.66, H 5.87, N 7.82; found: C 53.75, H 5.99, N 7.95. UV/Vis (CH_2Cl_2): λ_{max} (ε) = 1036 nm (590 M^{-1} cm^{-1}), 650 (785). IR (KBr): ν(V=O) 947, ν(V–O–V) 755 cm^{-1}. E_{pa} ($[OV^V(\mu\text{-}O_{oxo})(\mu\text{-}O_{phen})V^VO]^{3+}/[OV^{IV}(\mu\text{-}O_{oxo})(\mu\text{-}O_{phen})V^VO]^{2+}$): +0.55 V (irr); μ_{eff} = 1.79 BM.

$[V_2O_3L^9]$: Yield: 0.121 g (85%). $C_{30}H_{36}Cl_3N_4O_6V_2$ (757.5): calcd. C 47.5, H 4.88, N 7.39; found: C 47.64, H 4.96, N 7.54. UV/Vis (CH_2Cl_2): λ_{max} (ε) = 1032 nm (458 M^{-1} cm^{-1}), 665 (1217). IR (KBr): ν(V=O) 955, ν(V–O–V) 745 cm^{-1}. E_{pa} ($[OV^V(\mu\text{-}O_{oxo})(\mu\text{-}O_{phen})V^VO]^{3+}/[OV^{IV}(\mu\text{-}O_{oxo})(\mu\text{-}O_{phen})V^VO]^{2+}$): +0.49 V (irr); μ_{eff} = 1.75 BM.

$[V_2O_3L^{10}]$: Yield: 0.130 g (88%). $C_{32}H_{40}Cl_3N_4O_6V_2$ (784.5): calcd. C 48.94, H 5.09, N 7.14; found: C 49.12, H 5.21, N 7.25. UV/Vis (CH_2Cl_2): λ_{max} (ε) = 1036 nm (590 M^{-1} cm^{-1}), 650 (785). IR (KBr): ν(V=O) 958, ν(V–O–V) 748 cm^{-1}. E_{pa} ($[OV^V(\mu\text{-}O_{oxo})(\mu\text{-}O_{phen})V^VO]^{3+}/[OV^{IV}(\mu\text{-}O_{oxo})(\mu\text{-}O_{phen})V^VO]^{2+}$): +0.56 V (irr); μ_{eff} = 1.72 BM.

Acknowledgments

Financial support from the Council of Scientific and Industrial Research [Project Number: 01(2015)/05/EMR-II], New Delhi, India is gratefully acknowledged. We are also thankful to DST for the data collection on the CCD facility setup (Indian Institute of Science, Bangalore, India) under IRHPA-DST program. Authors are also thankful to Dr. Swapan K. Pati, Jawaharlal Nehru Centre for Advanced Scientific Research, Bangalore, India, for his help regarding the DFT study.

[1] a) M. Mahroof-Tahir, A. D. Keramidas, R. B. Goldfrab, O. P. Anderson, M. M. Miller, D. C. Crans, *Inorg. Chem.* **1997**, *36*, 1657; b) E. P. Copeland, I. A. Kahwa, J. T. Mague, G. L. McPherson, *J. Chem. Soc. Dalton Trans.* **1997**, 2849.
[2] J. C. Pessoa, M. J. Calhorda, I. Cavaco, I. Correia, M. T. Duarte, V. Felix, R. T. Henriques, M. F. Piedade, I. Tomaz, *J. Chem. Soc. Dalton Trans.* **2002**, 4407.
[3] S. Ghosh, K. K. Nanda, A. W. Addison, R. J. Butcher, *Inorg. Chem.* **2002**, *41*, 2243.
[4] S. K. Dutta, S. Samanta, S. B. Kumar, O. H. Han, P. Burckel, A. A. Pinkerton, M. Chaudhury, *Inorg. Chem.* **1999**, *38*, 1982.
[5] R. A. Holwerda, B. R. Whittlesey, *Inorg. Chem.* **1998**, *37*, 64.
[6] S. Mondal, P. Ghosh, A. Chakravorty, *Inorg. Chem.* **1997**, *36*, 59.
[7] D. Schulz, T. Weyhermüller, K. Wieghardt, B. Nuber, *Inorg. Chim. Acta* **1995**, *240*, 217.
[8] J. Chakravarty, S. Dutta, A. Chakravorty, *J. Chem. Soc. Dalton Trans.* **1993**, 2857.
[9] J. C. Silva, J. A. L. Pessoa, A. L. Vieira, L. Vilas-Boas, P. Ó. Brien, *J. Chem. Soc. Dalton Trans.* **1992**, 1745.
[10] J.-P. Launay, Y. Jeannin, M. Daoudi, *Inorg. Chem.* **1985**, *24*, 1052.
[11] A. Kojima, K. Okazaki, S. Ooi, K. Saito, *Inorg. Chem.* **1983**, *22*, 1168.
[12] F. Babonneau, C. Sanchez, J. Livage, J. P. Launay, M. Daoudi, Y. Jeannin, *Nouv. J. Chim.* **1982**, *6*, 353.
[13] M. Nishizawa, K. Hirotsu, S. Ooi, K. Saito, *J. Chem. Soc. Chem. Commun.* **1979**, 707.
[14] T. L. Riechel, D. T. Sawyer, *Inorg. Chem.* **1975**, *14*, 1869.
[15] A. Mondal, S. Sarkar, D. Chopra, T. N. Guru Row, K. Pramanik, K. K. Rajak, *Inorg. Chem.* **2005**, *44*, 703.
[16] R. W. Fessenden, *J. Chem. Phys.* **1962**, *37*, 747.
[17] A. Togni, G. Rist, G. Rihs, A. Schweiger, *J. Am. Chem. Soc.* **1993**, *115*, 1908.
[18] D. Kivelson, *J. Chem. Phys.* **1960**, *33*, 1094.
[19] J. H. Freed, G. K. Fraenkel, *J. Chem. Phys.* **1963**, *39*, 326.
[20] R. Wilson, D. Kivelson, *J. Chem. Phys.* **1966**, *44*, 154.
[21] B. S. Prabhananda, *Molecules Molec. Phys.* **1979**, *38*, 209.
[22] R. Das, B. S. Prabhananda, *J. Magn. Reson.* **1983**, *54*, 89.
[23] a) J. E. Wertz, J. R. Bolton, *Electron Spin Resonance*, McGraw Hill, New York, **1972**, p. 208–210; b) J. R. Pilbrow, *Transition Ion Electron Paramagnetic Resonance*, Clarendon Press, Oxford, **1990**, p. 339.
[24] M. B. Robin, P. Day, *Adv. Inorg. Chem. Radiochem.* **1967**, *10*, 247.
[25] K. Y. Wong, P. N. Schatz, *Prog. Inorg. Chem.* **1981**, *28*, 369.
[26] R. A. Rowe, M. M. Jones, *Inorg. Synth.* **1957**, *5*, 113.
[27] R. Kannappan, R. Mahalakshmy, T. M. Rajendiram, R. Venkatesan, P. Sambasiva Rao, *Proc. Indian Acad. Sci. (Chem. Sci.)* **2003**, *115*, 1.
[28] B. S. Furniss, A. J. P. W. G. Hannaford, Smith, A. R. Tatchell, in *Vogel's Textbook of Practical Organic Chemistry*, Pearson Education, Singapore, **2004**, p. 395–412.
[29] G. K. Lahiri, S. Bhattacharya, B. K. Ghosh, A. Chakravorty, *Inorg. Chem.* **1987**, *26*, 4324.
[30] R. Das, B. Venkataraman, V. R. Bhagat, A. S. Ghangrekar, T. Kuruvilla, B. K. Chaturvedi, G. S. Isola, B. M. Marwaha, P. G. Nair, R. S. Parolia, B. K. Sarkar, *Pramana – J. Phys.* **1986**, *27*, 661.
[31] R. Das, B. Venkataraman, *Res. Chem. Intermed.* **2005**, *31*, 167.
[32] J. E. Wertz, J. R. Bolton, in: *Electron Spin Resonance – Elementary Theory and Practical Applications*, McGraw-Hill Book Company, New York, **1972**, p. 465.
[33] M. J. Frisch, G. W. Trucks, H. B. Schlegel, G. E. Scuseria, M. A. Robb, J. R. Cheeseman, J. A. Montgomery Jr, T. Vreven, K. N. Kudin, J. C. Burant, J. M. Millam, S. S. Iyengar, J. Tomasi, V. Barone, B. Mennucci, M. Cossi, G. Scalmani, N. Rega, G. A. Petersson, H. Nakatsuji, M. Hada, M. Ehara, K. Toyota, R. Fukuda, J. Hasegawa, M. Ishida, T. Nakajima, Y. Honda, O. Kitao, H. Nakai, M. Klene, X. Li, J. E. Knox, H. P. Hratchian, J. B. Cross, C. Adamo, J. Jaramillo, R. Gomperts, R. E. Stratmann, O. Yazyev, A. J. Austin, R. Cammi, C. Pomelli, J. W. Ochterski, P. Y. Ayala, K. Morokuma, G. A. Voth, P. Salvador, J. J. Dannenberg, V. G. Zakrzewski, S. Dapprich, A. D. Daniels, M. C. Strain, O. Farkas, D. K. Malick, A. D. Rabuck, K. Raghavachari, J. B. Foresman, J. V. Ortiz, Q. Cui, A. G. Baboul, S. Clifford, J. Cioslowski, B. B. Stefanov, G. Liu, A. Liashenko, P. Piskorz, I. Komaromi, R. L. Martin, D. J. Fox, T. Keith, M. A. Al-Laham, C. Y. Peng, A. Nanayakkara, M. Challacombe, P. M. W. Gill, B. Johnson, W. Chen, M. W. Wong, C. Gonzalez, J. A. Pople, *Gaussian 03, Revision B.05*, Gaussian, Inc., Pittsburgh PA, **2003**.
[34] Bruker software: *SMART, SAINT, SADABS, XPREP, SHELXTL*, Bruker AXS Inc., Madison, Wisconsin, USA, **2004**.
[35] G. M. Sheldrick, SHELXL97, *Program for Crystal Structure Refinement*, University of Göttingen, Germany, **1997**.
[36] C. K. Johnson, ORTEP. Report ORNL-5138; *Oak Ridge National Laboratory*: Oak Ridge, TN, **1976**.

Received: August 26, 2005
Published Online: March 16, 2006

